한국윤활학회지(1995), 제 11 권 제 5 호
Journal of KSTLE(1995) Vol. 11, No. 5, pp.40~46

Surface Wear Monitoring with a Non-Vibrating Capacitance Probe

E. S. Zanoria, K. Hamall, S. Danyluk[1] and A.L. Zharin[2]

[1]*The George W. Woodruff School of Mechancial Engineering, Georgia Institute of Technology Atlanta, Georgia, U.S.A.,*
[2]*Belarussian Powder Metallurgy Association, Minsk, Belarus*

Abstract—This study concerns the design and development of the non-vibrating capacitance probe which could be used as a non-contact sensor for tribological wear. This device detects surface charge through temporal variation in the work function of a material. Experiments are performed to demonstrate the operation of the probe on a roating aluminum shaft. The reference electrode of the probe, made of lead, is placed adjacent (<1.25-mm distance) to the shaft. Both surfaces which are electrically connected, form a capacitor. An artificial spatial variation in the work function is imposed on the shaft surface by coating a segment along the shaft circumference with a colloidal silver paint. As the shaft rotates, the reference electode senses changing contact potential difference with the shaft surface, owing to compositional variation. Temporal variation in the contact potential difference induces a current through the electrical connection. This current is amplified and converted to a voltage signal by an electoronic circuit with an operational amplifier. The magnitude of the signal decreases asymptotically with the electrode-shaft distance and increases linearly with the rotational frequency. These results are consistent with the theoretical model. Potential applications of the probe on wear monitoring are proposed.

1. Introduction

Mechanical systems such as heat combustion engines have components that are dynamically in contact with another body. These components are subjected to cyclic motions that could involve impact loading, shear straining, plastic deformation, frictional heating and fatigue of subsurface regions. A combination of these mechanisms leads to surface damage that impairs the performance of the component. In addition, the chemical interaction between the component surface and surrounding fluids could also accelerate suface degradation. Such problems, if unattended, could result in catastrophic malfunction of the machine and even compromise operational safety. in this regard, it is desirable to monitor the surface condition of a critical tribocomponent. The design of the sensors to monitor the operation of machinery depends largely on the nature of tribological application.

This paper will present a preliminary evaluation of a surface-monitoring method that exploits the spatial variation in the work function of a material. The work function refers to an energy barrier to prevent the escape of electrons from the surface. it is governed by the physio-chemical nature of the surface and also depends on the environmental conditions. From a tribological standpoint, the work function is a useful parameter for evaluating mechanical deformation features such as dislocation pile-ups and residual stresses. For example, Craig and Radeka (1969) have demonstrated that a metal subjected to different degrees of compressive stress, exhibits a variation in the work function.

The present study focuses on the design and development of a non-vibrating capacitance probe as modified from that of the Kelvin-Zisman method (Zisman, 1992) that uses a variable capacitor to measure the contact potential difference (CPD) between two surfaces. This paper provides a description of the Kelvin-Zisman method to monitor surface probe, and demonstrates the operation of the probe on a rotating shaft.

2. Theoretical Background

2-1. Kelivin-Zisman Probe

This technique is done by creating a parallel plate

capacitor and vibrating one plate (reference electorde) relative to the surface of interest, as shown in Fig1. The vibration induces a current flow which can be described in terms of the geometry of the dynamic capacitor and difference in work function between the surfaces. If the work function of the reference electrode (φ_{ref}) is known, then the changes in the work function of the other surface ($\varphi_{desired}$) can be related to whatever experimental conditions are chosen. The general equation for the induced current (Diefenderfer, 1972) is

$$i = V(dC/dt)+C(dV/dt) \quad (1)$$

where V, the CPD voltage, is defined by

$$V = (\varphi_{ref} - \varphi_{desired})/e \quad (2)$$

and C, the capacitance, is expressed as

$$C = \varepsilon_r\varepsilon_o A/d, \quad (3)$$

e is the charge of an electron, ε_r is the relative dielectric constant, ε_o is the permitivity in free space, A is the area of the reference electrode and d is the spacing between the surfaces.

A typical experimental condition involves a reference electrode that does not dtect a varying $\varphi_{desired}$, thus, the term dV/dt in equation 1 is assumed to be zero. In most CPD-measurement studies (Anderson and Alexander, 1952; Baumgartner and Leiss, 1988), such a condition is implemented by having the vibrating reference electrode fixed in position on a particular site of the sample surface. The induced current is contributed solely by the change in the capacitance owing to the sinusoidal variation in d expressed as

$$d = d_o+d_i\sin\varpi t \quad (4)$$

where d_o is the mean spacing, d_i is the amplitude, ϖ is the angular frequency and t is the time. Substituting this equation to equations 3 and 1 yielde

$$i = -V\varepsilon_r\varepsilon_o A d_i\cos\varpi t/(d_o+d_i\sin\varpi t)^2 \quad (5)$$

The kelvin-Zisman technique to measure V is to provide a compensating voltage (V_c) to the virbrating capacitor (Fig. 1) so that i=0. The dc voltage could be applied either externally (Wolff *et al.*, 1969; de Boer *et al.*, 1973) or through a feedback circuit via a phase sensitive detector (Harris and Fiasson, 1984).

2-2. Non-vibrating Capacitance Probe

This probe also forms a capacitor between the reference electrode and surface of interest. However, the spacing between the two surfaces is fixed. Instead of the variable capacitance, the current is induced by the temporal change in CPD. In reference to equation 1, the formulation for the induced current is simplified to

$$i = C\ (dV/dt) \quad (6)$$

Varying the CPD with time could be achieved by imposing a lateral displacement between the reference electrods and a samle surface with heterogeneous work function. A combination of this equation with euation 3 which yields

$$i = \varepsilon_r\varepsilon_o A(dV/dt)/d, \quad (7)$$

suggests that the magnitude of the induced current decreases asymptotically with the capacitor spacing, and increases with the area of the reference electorde and the rate of CPD change. The present study involves the scanning of a cylindrical surface rotating along its longitudinal axis (Fig. 2).

Using the geometry depicted in Fig2, assume that, along the circumference of the cylinder, part of the surface consists of material A and the rest, of material B; each material has a unique work function.

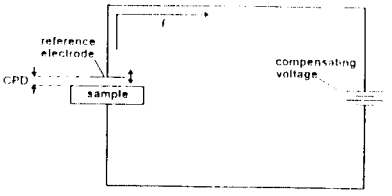

Fig. 1. A schematic of the Kelvin-Zisman method.

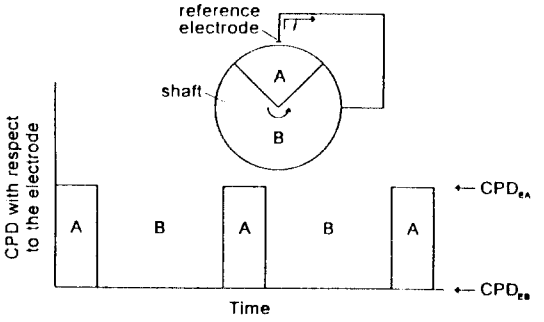

Fig. 2. CPD variation between the reference electrode and rotating cylindrical surface composed of materials A and B.

As the cylinder rotates at a constant speed, the reference electrode senses a contact potential difference with material A (CPD_{EA}) and another potential with material B (CPD_{EB}). Also assume that CPD_{EB} is zero. The variation in the CPD with time can be described by a rectangular wave function V(t) with an amplitude CPD_{EA} (Fig. 2). The Fourier series of the function is

$$V(t) = V'x + V'/\Pi\{\sum[(\sin(2\Pi nx)/n)\cos(w\Pi ft)] + [(1-\cos(w\Pi nx)/n)\sin(2\Pi ft)]\} \quad (8)$$

whereby $V' = CPD_{EA} - CPD_{EB}$ (in volts), f is the fundamental frequency which is equivalent to the rotational frequency, x is the ratio of the arc length of A to the circumference of the cylinder and n=1, 2, 3,....∞. The derivative of this function is defined by

$$dV/dt = -2V'f\{\sum[(\sin(e\Pi nx)/n)\sin(2\Pi ft)] + [(1-\cos(2\Pi nx)/n)\cos(2\Pi ft)]\} \quad (9)$$

For $CPD_{EB} \neq 0$, the derivative of V(t) is still identical to equation 9 where the dc component is eliminated.

Fig. 3 shows plots of equation 9 for x values of 0.013 and 0.3. For these calculations, V'=1, f=15 Hz and n=1 to 10. Each cycle of the wave consists of two major peaks, one with positive (maximum) and the other with negative (minimum) value. These peaks define the boundaries of material A where there are sharp changes in the CPD. The gap between the peaks widens as the length fraction of A increases.

Equation 9 indicates that the magnitude of the peak depends on the fundamental frequency. This is illustrated in Fig. 4 that reveals a linear increase in maximum dV/dt from 10 to 20 Hz. For this plot, x is fixed at 0.013 and V' and n are the same as above.

Take note that waves with smaller amplitude separate the major peaks as shown in Fig. 3. There should be a straight line (dV/dt=O) instead because of the absence of CPD variation between material boundaries. The appearance of minor waves between the large peaks is attributed to the limited number of harmonics included in the calulation. With higher number of harmonics, the amplitude of these waves aspproaches to zaeo.

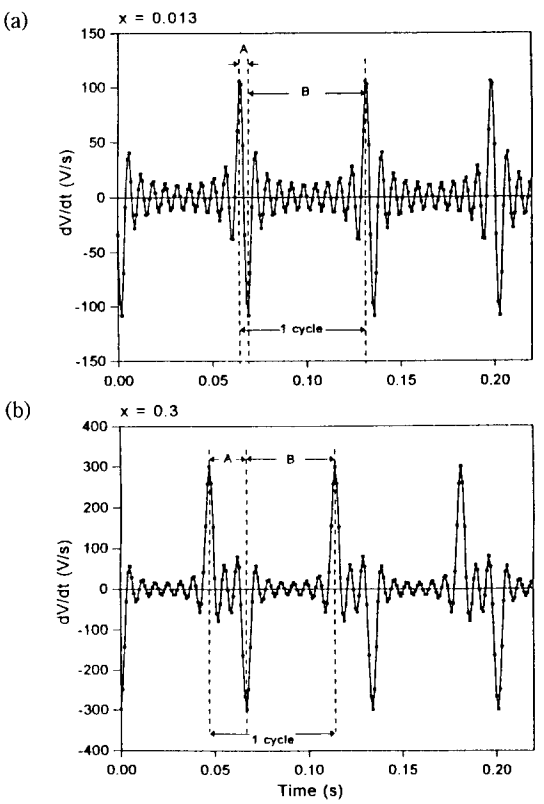

Fig. 3. A theoretical variation of dV/dt with time.

3. Experiment

3-1. Set-up

The apparatus conisisted of an aluminum shaft (length=432 mm, diameter = 50.8 mm) rotated by a stepper motor (Fig. 5). Both ends of the shaft were supported by roller bearings. One end was con-

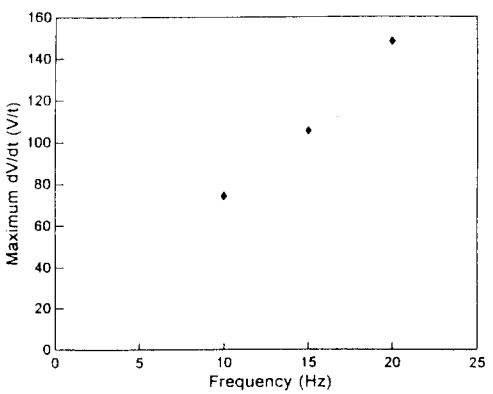

Fig. 4. Theoretical maximum dV/dt plotted as a function of frequency.

nected to the motor spindle with a coupling. Interfaced with the motor is a control box for regulating the rotational speed. The entire mechanical assembly was mounted on a vibration-isolation table. The rotational frequency of the shaft which was monitored by a tachometer, was set at 10, 15, 20 and 25 Hz (or 600, 900, 1200, 1500 rpm).

The non-vibrating capacitance probe was mounted on an xyz positioning system which was mechanically isolated from the above set-up. Stepper motors control the lateral motion of the probe along the longitudinal axis of the shaft and the vertical position. The probe was positioned such that the reference electrode was perpendicular to the shaft surface. A separate positioning stage with a translational resolution of 0.01 mm was used to manually adjust the spacing between the shaft and the reference electrode. Spacings ranging from 0.1 to 1.25 were used.

Artificial variation in the work function was imposed on the sample surface by coating a segment along the shaft circumference (Fig. 5) with a colloidal silver paint (Ted Pella, Inc.). Most of the tests were conducted for a silver strip with an arc length that was 1.3/100 (or 0.013) of the circumferencial length of the shaft. One test was performed for a separate coating with a length fraction of 0.3. The coating strips were approximately 14-μm thick and 5-mm wide.

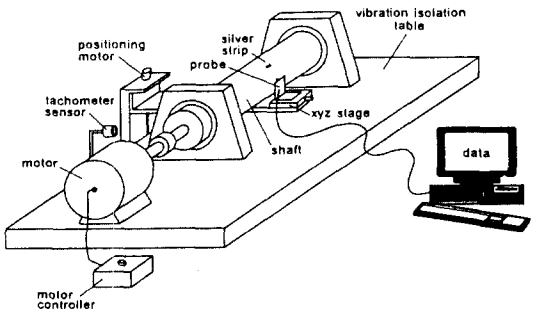

Fig. 5. Experimental set-up.

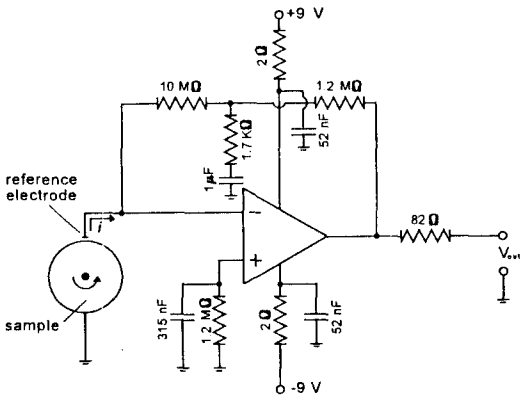

Fig. 6. Circuit diagram of the non-vibrating capacitance probe.

3-2. Signal Processing

The reference electrode of the probe was made of lead wire with a cross-sectional area of approximately 0.446 mm^2. Electrical connection between the sample and the common ground of the probe's electronic circuit, was maintained through a brush in contact with the shaft. The current induced by the time-varying CPD between the electrode and rotating shaft surface was converted to a voltage output (Fig. 6) via a high ohmic circuit with a gain factor of 3.9×10^9V/amp. The operational amplifier in the circuit received a dc power of ± 9 V. The voltage ouput of the amplifier is recorded by a data acquisition system (Data Translation 2831) at a rate of 10 kHz.

4. Results

Fig. 7a shows an example of signal output for the silver strip with a length fraction of 0.013. The signal exhibits a series of large waves, separated by fluctuations with smaller amplitudes. This pattern is identical to that of the theoretical signal which is calculated for similar length fraction (Fig. 3a). The time interval between the large waves corresponds to the rotational frequency of the shaft. The interval between the maximum and minimum peaks of each wave packet represents the traverse of the probe along the arc length of the silver strip. The model in Fig. 2 indicates that upon entry into the silver strip, the reference electrode senses an abrupt shift in the contact potential difference from aluminum to silver. At this point, the rate of change in CPD, i.e., dV/dt, is maximum (equation 7). As the reference electrode exits from silver to aluminum, it senses another sharp change in CPD but with a dV/dt of reverse polarity. In accordance to this model, the interval between the maximum and minimum points of the large peaks is longer for the silver strip with a length fraction of 0.3 (Fig. 7b).

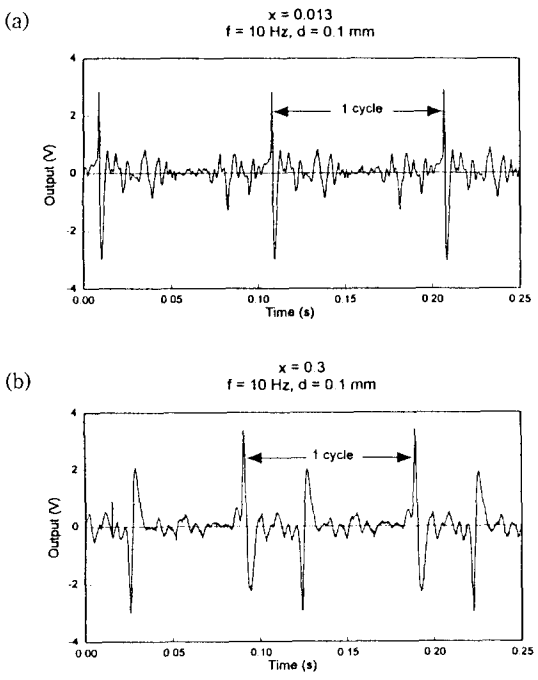

Fig. 7. Samples of probe output signal.

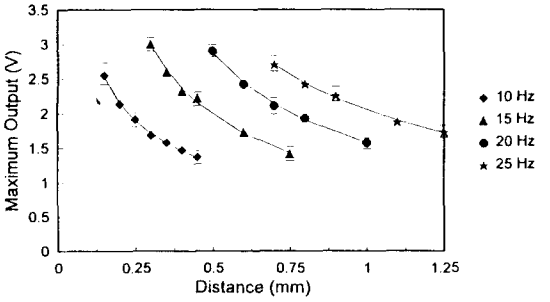

Fig. 8. Magnitude of maximum output plotted as a function of probe-sample distance.

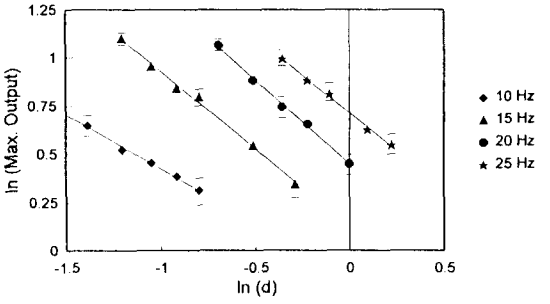

Fig. 9. Linearized plot of maximum output vs. distance.

Table 1. Experimental values of c and s

Frequency (Hz)	c	s
10	0.874	0.6
15	1.130	0.8
20	1.565	0.9
25	2.040	0.8

As mentioned earlier, an interval of minor waves separates the large ones as shown in Fig. 7a. This interval could be the electrical signature of uncoated aluminum. The fluctuation could reflect microstructural variation in the aluminum surface that also gives rise to heterogeneity in the work function. The microstructural variation could be linked to the machining history of the shaft. Since this study concerns only with variation in surface composition rather than microstructure, less emphasis will be given on the minor waves.

The amplitudes of both the maximum and minimum peaks of the major wave is influenced strongly by the rotational frequency of the shaft and the capacitance spacing. As an example, a quantitative analysis of the maximum peak measured for a silver strip with a length fraction of 0.013, will be presented. Fig. 8 shows that the magnitude of the maximum peak declines non-linearly from 2.8 to 0.9 V with probe distance. It should also be noted that the curves in this diagram have identical shape, however, they shift to higher voltages as the rotational frequency increases from 10 to 25 Hz.

A mathematical equation for each curve in Fig. 8 could be derived by linearization. This is done by plotting the natural logarithm of the maximum voltage (V_{max}) against that of the distance, and then calculating the slope (s) and y-intercept (y) through linear regression. Fig. 9 reveals that the fit (r^2) of the linearized curves ranges from 0.99 to 1.00. Such excellent r^2 values confirms the validity of the curve fitting technique being applied. Rearranging the linear equation

$$\ln(V_{max}) = [s \; x \; \ln(d)]+y \tag{10}$$

yields an asymptotic expression for V_{max}

$$V_{max} = c/d^s \tag{11}$$

where $c=e^y$. Equation 11 takes into account the negative slope indicated by the linearized plots in Fig. 9 Table 1 shows the values of c and s for each rotational frequency.

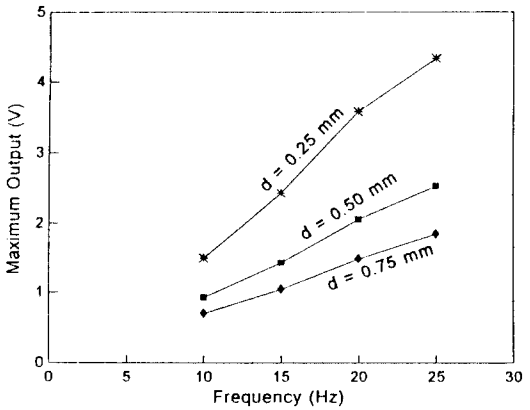

Fig. 10. Magnitude of maximum output plotted as a function of rotational frequency.

The empirical equation for V_{max} conforms with the predicted model for the induced current (equation 7). Both equations are asymptotic, however, the experimental values of s in equation 9 range from 0.6 to 0.9. Except for f=10 Hz, these values are slightly below 1 which is the predicted value. It should be noted that the probe signal is acquired through current-to-voltage conversion circuit a gain factor of 3.9×10^5 V/amp. Taking these facts and equation 7 into account, the authors propose that the numerator, c, in the empirical equation represents a product of the induced current, conversion factor, dielectric constants and dV/dt. Among these parameters, dV/dt which increases linearly with the rotational frequency (Fig. 4), is variable. Fig. 10 shows that, at a constant d, the magnitude of the maximum peak increases linearly with the rotational frequency and the slope for each line increases with decreasing spacing distane.

5. Discussion/Conclusion

This study has demonstrated the applicability of the non-vibrating capacitance probe for detecting surface variation in the work function. This variation is reflected by the nature of the current induced by the changing contact potential difference between the reference electrode and the surface in question. The magnitude of the induced current which indicates the sensitivity of the probe, decreases asymptotically with distance between the probe and sample, and it increases linearly with the rate of CPD change. These results are consistent with the theoretical model.

A potential application of the non-vibrating capacitance probe is for detecting surface wear of an object subjected to sliding contact. Based on the results of this study, one technique is to apply a thin coating on the sliding body that is compositionally different from the substrate. Partial removal of this coating due to sliding contact creates sites where the substrate material is exposed. Formation of these sites create lateral compositional variation, thus, heterogeneity in the work function of the wear surface. This yields an induced-current pattern that is unqiue from that of the unworn surface coating.

Another method which does not require surface coating on the sliding object, is to detect directiy the changes in the surface microstructure of the sliding body. Fig. 7 shows that the microstructural variation on the aluminum shaft. It should be noted, however, that the magnitude of current induced by microsctructural variation is lower than that produced by compoitional variation, by about a factor of three.

Acknowledgment

Part of this work was supported by the U.S. Office of Naval Research, Contracts N00014-95-1-0903 and N00014-94-1-1074. Thanks are extended to Dr. Peter Schmidt for this encouragement and support. This work is the outgrowth of a project supported by the U.S. National Science Foundation. We thank Dr. Jorn Larsen-Basse for his support. The authors also express thanks to Ligang Xu for technical help during this project.

References

1. Craig. P. P. and Radeka, V., "Stress Dependence of Contact Potential: The ac Kelvin Method," *Rev. Sci. Instrum.*, Vol.41, pp.258-264, 1969.
2. Zisman, W. A., "A New Method of Measuring Contact Potential Differences in Metals," *Sci. Instrum.*, Vol.3, pp.367-370, 1932.
3. Diefenderfer, A. J., *Principles of Electronic Instrumentation*: W. B. Saunders Company, Philadelphia, 1972.
4. Anderson, J. R. and Alexander, A. E., "Theory of the Vibrating Condenser Converter and Application to Contact Potential Measurements," *Aus. J. Appl. Sci.*, Vol.3, pp.201-209, 1952.

5. Baumgartner, H. and Leiss, H. D., "Micro Kelvin Probe for Local Work-function Measurements," *Rev. Sci. Instrum.*, Vol.59, pp.802-805, 1988.
6. Wolff, M., Guile, A. E., and Bell, "Measurement of Localized Surface Potential Difference," *J. Phys. E: Sci. Instrum.*, Vol.2, pp.921-924, 1969.
7. de Boer, J. S. W., Krusemeyer, H. J., and Burhoven Jaspers, N. C., "Analysis and Improvement of the Kelvin Method for Measuring Differences in Work Function," *Rev. Sci. Instrum.*, Vol.44, pp. 1003-1008, 1973.
8. Harris, L. B. and Fiasson, J., "Vibrating Capacitor Measurement of Surface Charge," *J. Phys, E: Sci, Instrum.*, Vol.17, pp.788-792, 1984.